Probe the spin-reorientation transition with magnetic susceptibility—a theoretical analysis

Cite as: J. Appl. Phys. **109**, 113902 (2011); https://doi.org/10.1063/1.3590709
Submitted: 15 March 2011 . Accepted: 12 April 2011 . Published Online: 02 June 2011

B. F. Miao, L. Sun, B. You, An Hu, and H. F. Ding

Probe the spin-reorientation transition with magnetic susceptibility—a theoretical analysis

B. F. Miao, L. Sun,[a] B. You, An Hu, and H. F. Ding[b]
National Laboratory of Solid State Microstructures and Department of Physics, Nanjing University, 22 Hankou Rd., Nanjing 210093, China

(Received 15 March 2011; accepted 12 April 2011; published online 1 June 2011)

We investigated the thickness-driven spin-reorientation transition (SRT) between in-plane and perpendicular easy axes in ultrathin magnetic films. Coherent rotation model calculations show that one can distinguish transition pathways via a canted state from those involving a state of coexisting phases by utilizing magnetic susceptibility measurements. Surface/interface anisotropy constants and the influence of external fields on the SRT are also explored. Quantitative agreement between the experiment and our model is shown for the Co/Au(111) system. © *2011 American Institute of Physics*. [doi:10.1063/1.3590709]

I. INTRODUCTION

Ultrathin magnetic films have been intensively studied for fundamental and technological interests in the last several decades. Magnetic anisotropy is one of the main topics in this field as it governs the sample magnetization orientation. When the film thickness (t) is in the ultrathin region, the surface/interface contribution to its properties may become dominant and lead to novel phenomena, such as enhanced anisotropy and change of the easy axis of magnetization, i.e., the spin reorientation transition (SRT). The SRT can be induced by a change of temperature (T) or t. The t-driven SRT is of special interest due to its impact for high-density magnetic data storage.[1–3] The SRT proceeds from perpendicular to in-plane magnetic spin orientation with increasing t in Fe/Cu(001),[4] Fe/Ag(100),[5,6] Fe/Au(001),[7] and Co/Au(111) (Refs. 2 and 8–12) systems but is opposite for Ni/Cu(001) system, proceeding from in-plane to perpendicular spin orientation with increasing t in the monolayer range.[13,14]

Magnetic susceptibility, defined as $\chi = dM/dH$, where M is the magnetization and H is the applied magnetic field, has been widely used to explore the Curie transition at temperature T_c between ferromagnetic and paramagnetic phases.[15] This transition features a pronounced susceptibility peak that can be readily detected via a field-modulation technique. The magneto-optical Kerr effect (MOKE) has been used to probe χ for ultrathin films[16] and has been extended to investigate the temperature-driven SRT.[17,18] In particular, we focus on the study by Pütter *et al.*[19] of the thickness dependent SRT for Co/Au(111) monitored during film growth via MOKE χ measurements. They reported an interesting observation that χ exhibits two peaks when the *ac* modulation field is applied perpendicular to the sample plane, while only a single broad peak with the in-plane *ac* field.[19] A quantitative understanding of this observation, however, is absent.

To unveil the mechanism underlying this intriguing observation, we calculate χ in the vicinity of the SRT with increasing film thickness utilizing the coherent rotation model. We find that one can distinguish transition pathways involving a canted state from those involving a state of coexisting phases. Our calculations also show that one can readily extrapolate first- and second-order surface anisotropy constants from the peak positions in χ. From a fitting of χ-curves, one can obtain the evolution of the ratio between perpendicular and in-plane components of M across the SRT through the coexistent region. With additional *dc* bias field, one can also estimate the in-plane magnetic anisotropy constant. The feasibility of the calculations are demonstrated for the well-known Co/Au(111) system, where good agreement is obtained.

For an ultrathin film, the free energy F_A can be simplified by neglecting the in-plane anisotropy:

$$F_A = \tilde{K}_1 \sin^2(\theta) + K_2 \sin^4(\theta), \tag{1}$$

where $\tilde{K}_1$ and K_2 are first- and second-order thickness- and temperature-dependent anisotropy coefficients, and θ is the angle between the surface normal **n** and the direction of M. $\tilde{K}_1$ contains the shape anisotropy:

$$\tilde{K}_1 = K_1 - \frac{1}{2}\mu_\circ M^2. \tag{2}$$

The energy phase diagram has been described by Millev *et al.*[20,21] To elucidate the SRT-induced behavior of χ, we summarize their main results. Minimizing the free energy with respect to θ yields three solutions for the equilibrium angle $\sin^2(\theta_{eq}) = 0, 1$, and $-\tilde{K}_1/2K_2$, correspond to vertical, in-plane, and canted phases, respectively. The vertical phase is stable for $\tilde{K}_1 > 0$, the in-plane phase is stable for $K_2 < -\tilde{K}_1/2$, and the canted phase for $\tilde{K}_1 < 0$ and $K_2 > -\tilde{K}_1/2$ (see Fig. 1). The most interesting feature of the anisotropy space is that there is a region where the vertical and in-plane phases can coexist. It is located in the fourth quadrant, with $\tilde{K}_1 = 0$ and $K_2 = -\tilde{K}_1/2$ as the two boundaries. For clarity, we insert typical angle-dependent energies in the four regions. For the vertical and in-plane regions, the angle dependent energy plots have only one energy minimum at 0° and 90°, respectively. For the canted state, there

[a]Electronic mail: lsun@nju.edu.cn.
[b]Electronic mail: hfding@nju.edu.cn.

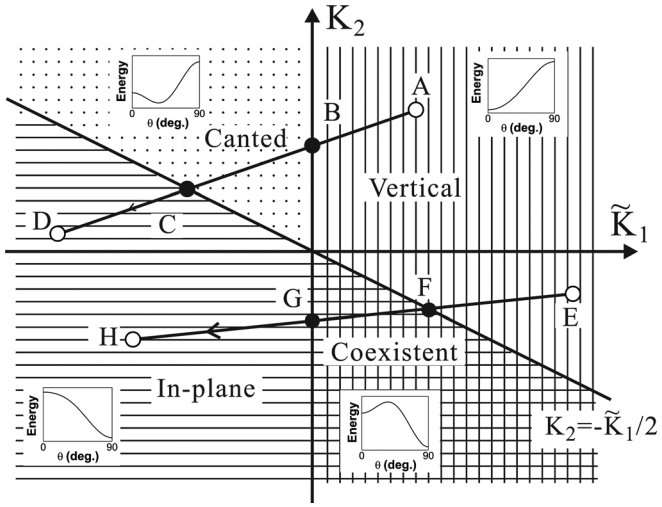

FIG. 1. The energy phase diagram in the anisotropy space. The insets show a typical angle-dependent energy of each state. Linear trajectory AD and EH represent thickness-driven SRT via a canted state and a coexistent state, respectively.

is also only one energy minimum, located at an arbitrary angle between 0° and 90°. However, for the coexistent state the energy plot has two minima, one at 0° and the other at 90°.

To investigate the thickness-driven SRT quantitatively, the dependence of K_i on the magnetic film thickness t is needed. The most widely used phenomenological ansatz for the separation of volume and surface contributions was proposed by Gradmann,[11,22,23] as

$$K_i(t,T) = K_{ib}(T) + \frac{K_{is}(T)}{t}, i = 1,2, \tag{3}$$

where the subscript b is for bulk and s is for the surface and interface contributions to K_1 and K_2. Within the framework of "anisotropy flow",[11,20,21] one can describe a t-driven SRT by plotting the trajectory $\{\tilde{K}_1(t,T), K_2(t,T)\}_{T=const.}$ in a $\tilde{K}_1 - K_2$ diagram. The diagram identifies three generic cases depending on the sign of K_2 at the transition. The transition from vertical to in-plane magnetization occurs via a continuous canting of M when $K_2 > 0$ (e.g., linear trajectory AD in Fig. 1), or it directly changes from the vertical to the in-plane direction when $K_2 = 0$. The third situation is for $K_2 < 0$, where the transition proceeds via a state of coexisting phases (e.g., linear trajectory EH in Fig. 1).

For the Co on Au(111) system, two opposing results have been reported. Allenspach *et al.*[8] and Popov *et al.*[24] reported that the SRT takes place by a continuous rotation, while Oepen *et al.*[11] and Ding *et al.*[12] provided evidence for a state of coexisting phases. We performed $\chi(t)$ calculations utilizing the coherent rotation model and find that the two kinds of SRT can be distinguished. We also demonstrate that the surface anisotropy constants can be extracted from the positions of peaks in χ.

The paper is organized as follows. In Sec. II, a generalized representation is given of the thickness-driven SRT utilizing dimensionless parameters. We show that $\chi(t)$ behaves differently depending on whether the SRT pathway is via a canted state or a coexistent state. In Sec. III, we apply our model to the Co/Au(111) system and clarify the debate about the transition pathway. Knowing the bulk anisotropy constants for Co, the surface anisotropy constants for Co/Au(111) can be estimated from the peak positions of χ. We also discuss the influence of the in-plane anisotropy of Co and of external fields on SRT. Finally, a summary of the main results is presented in Sec. IV.

II. GENERALIZED REPRESENTATION OF SRT

In a measurement of χ, a small modulation field is applied. The response depends on the orientation of the modulation field. We will discuss the cases for an *ac* field applied in either perpendicular or in-plane direction. First, we discuss the case in perpendicular applied field ($H_\perp$). The free energy can be written as:

$$F_A = \tilde{K}_1 \sin^2(\theta) + K_2 \sin^4(\theta) - \Delta H M \cos\theta, \tag{4}$$

where ΔH is the *ac* modulation field. The perpendicular and in-plane susceptibilities can be defined as:

$$\chi_\perp = \frac{\cos\theta_{\Delta H} - \cos\theta_{-\Delta H}}{2\Delta H} t, \tag{5}$$

$$\chi_= = \frac{\sin\theta_{\Delta H} - \sin\theta_{-\Delta H}}{2\Delta H} t. \tag{6}$$

The measured χ-signal depends linearly on the total magnetic moment. In ultrathin films, it is almost proportional to the film thickness.[25] In our calculations, dimensionless parameters are adopted to represent the SRT pathway proceeding via a canted state or coexistent state: $\tilde{K}_{1b} = -2$, $K_{1s} = 1$, $K_{2b} = -1$, $K_{2s} = 1$ or $\tilde{K}_{1b} = -1$, $K_{1s} = 1$, $K_{2b} = -2$, $K_{2s} = 1$, respectively. In the calculations within this section, M is set to 1, and $\Delta H = 0.001$. In the vicinity of the transition point, the angle dependent energy exhibits a nearly flat minimum. Therefore a small *ac* field will cause large oscillation of the direction of M, leading to a pronounced peak in χ. Figure 2(a) shows $\chi_\perp$ and $\chi_=$ during the SRT via a canted state. The sharp peak at $t_C = 0.75$ of $\chi_\perp$ represents the boundary between the canted and in-plane states (point C in Fig. 1). And $\chi_=$ exhibits two weaker peaks at $t_B = 0.5$ and $t_C = 0.75$ representing the two boundaries of the canted state (points B and C in Fig. 1). In the preceding text, we assume that the whole sample is in a single domain state. However, near the SRT, a multi-domain state is commonly found.[8,9,11,26] Thus we consider two oppositely tilted domains, magnetized along θ_0 and $-\theta_0$, respectively. Applying a field along **n** causes M to tilt, i.e., M for both domains rotate toward **n**. In such a case, $\chi_\perp$ remains in the **n** direction while $\chi_=$ is balanced by domains with opposite horizontal components. Therefore when the *ac* field is applied along **n**, only $\chi_\perp$ is detectable for the SRT via a canted state, and there is only a single peak.

Figure 2(b) shows $\chi_\perp$ with increasing t near the SRT for a pathway involving a coexistent state. When M is in the perpendicular state, a small field along **n** will not change its orientation, resulting $\chi_= = 0$. When M is in the sample plane, the in-plane component of M remains the same under a

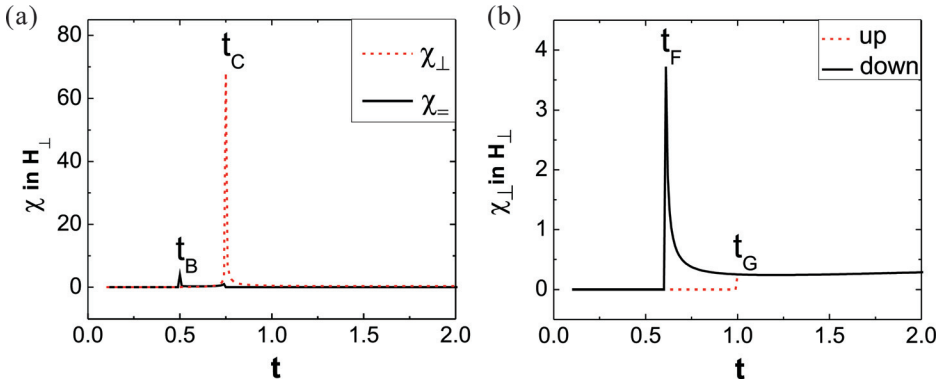

FIG. 2. (Color online) (a) Thickness dependence of the perpendicular (dashed line) and in-plane (solid line) susceptibilities around the SRT via a canted state. The *ac* modulation field is applied perpendicular to the sample plane. (b) The perpendicular susceptibility around the SRT via a coexistent state in perpendicular *ac* modulation field. Line up (dashed line) and down (solid line) represent that the magnetizations in the coexistent region orient either fully perpendicular or fully within the sample plane, respectively.

positive (ΔH) or a negative ($-\Delta H$) perpendicular field. As a result, $\chi_{=} \equiv 0$ during this evolution. Therefore we focus our discussion on $\chi_{\perp}$. In the coexistent state, both in-plane and perpendicular magnetic domains can exist. For simplicity, we discuss two extreme situations, where M is either in fully perpendicular (line up in Fig. 2(b)) or fully in-plane state (line down in Fig. 2(b)). The measured χ is a superposition of both situations. One can find that both cases show a single peak at a distinct thickness. The peak at $t_F = 0.6$ represents the emergence of the in-plane component of M (point F in Fig. 1), while peak at $t_G = 1.0$ represents the disappearance of the vertical component of M (point G in Fig. 1). The experimentally detected χ is a superposition of these two in Fig. 2(b). So if the proportion of in-plane to vertical magnetization in the coexistent region is proportionate, a double peak in χ is expected.

When the *ac* field is applied within the sample plane ($H_{=}$), the free energy can be written as:

$$F_A = \tilde{K}_1 \sin^2(\theta) + K_2 \sin^4(\theta) + \Delta H M \sin\theta. \qquad (7)$$

Similar to the preceding discussion, the perpendicular susceptibilities of the two kinds of SRT can be neglected when the *ac* modulation field is applied within the sample plane. Figure 3(a) shows $\chi_{=}$ during the SRT via a canted state. The single peak at $t_B = 0.5$ of $\chi_{=}$ represents the transition from vertical to canted state. Figure 3(b) shows $\chi_{=}$ for increasing t near a SRT that occurs via a coexistent state. Similar to the previous situation, two peaks at $t_F = 0.6$ and $t_G = 1.0$ appear when all components of M for the coexistent region are oriented in-plane or vertical, respectively. These two peaks appear at the same t-values as the SRT via coexistent state under perpendicular modulation field, representing the two boundaries of the coexistent region.

We now summarize the main features of the two kinds of t-driven SRT. For a SRT via a canted state, a single peak is expected under vertical or in-plane *ac* fields. They appear at different thicknesses representing two boundaries of the canted phase. When the bulk anisotropy constants are known, one can use these two peak positions to estimate the surface anisotropy constant according to Eq. (3). For a SRT via a coexistent state, if the ratio of in-plane to vertical magnetization is suitable, both susceptibilities in *ac* modulation fields oriented within or perpendicular to the sample may exhibit two peaks. The two peaks appear at the same thicknesses for the modulation field applied in both perpendicular and in-plane directions. They represent two boundaries of the coexistent region. Similarly, one can use these two peak positions to estimate the surface anisotropy constant as is discussed in the following text. Here we note that we mainly macroscopically discuss the systems with the possibility of forming magnetic domains. The detailed domain structures, such as the stripe domains, may also influence the susceptibility. This influence, however, can be neglected if the domain size is considerably larger than the domain wall width.

The SRT can be influenced by the externally applied field.[21,27] When a *dc* bias field is applied, the peaks in χ can appear at different t-values as is observed experimentally.[19] The bias field will favor the different phases according to the direction in which it is applied. For example, the two boundaries of the coexistent region shift toward the original in-plane/perpendicular region of M under a perpendicular/in-plane bias field, respectively. Interestingly, one boundary shifts more quickly than the other, and the coexistent region

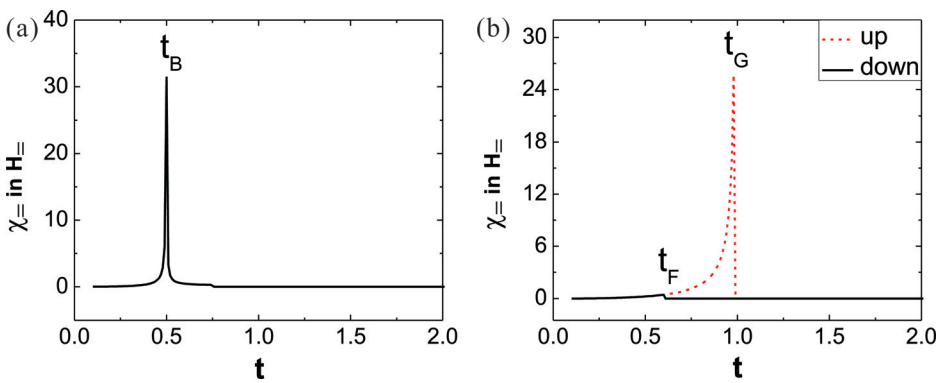

FIG. 3. (Color online) (a) Thickness dependence of the in-plane susceptibility $\chi_{=}$ around the SRT via a canted state. The *ac* modulation field is applied within the sample plane. (b) The in-plane susceptibility around the SRT via a coexistent state in in-plane modulation field. Line up (dashed line) and down (solid line) represent that the magnetizations in the coexistent region orient either fully perpendicular or fully within the sample plane, respectively.

becomes narrower with increasing bias field. The shift of the boundaries by the external field was calculated by Millev *et al.*[21] The two boundaries of the coexistent region in horizontal field can be calculated utilizing $(2\tilde{K}_1 + 4K_2) - HM = 0$ and $8\tilde{K}_1^3 + 27K_2H^2M^2 = 0$. $2\tilde{K}_1 + HM = 0$ and $8(\tilde{K}_1 + 2K_2)^3 - 27K_2H^2M^2 = 0$ are equations for obtaining the two boundaries under a perpendicular field. When the applied *dc* bias field is large enough, one of the phases can become unstable causing the state of coexisting phases to disappear, and then only a single peak in χ is expected. For $K_2 > 0$ (SRT via a canted state under zero bias field), the positions of the peaks in $\chi_\perp$ and $\chi_=$ will also collapse into the same thickness when the bias field is strong enough.

III. APPLICATION TO THE CO/AU(111) SYSTEM

In last section, we provided a general description of the *t*-driven SRT. Now we apply our model to the well-known Co/Au(111) system. In the experimental measurements, s-polarized light is used to minimize the influence of the transverse Kerr effect.[12,19,28] In this case, we only need to calculate the polar and longitudinal susceptibility (i.e., $\chi_\perp$ and $\chi_=$ discussed in last section) in our simulations. In the experiments, χ was found to exhibit peaks at 4.18 monolayer (ML) and 4.39 ML when the *ac* modulation field was applied along **n**, while a broad peak was detected at 4.39 ML under an in-plane *ac* field.[19] Based on the preceding discussion, one can conclude that the *t*-driven SRT in Co/Au(111) proceeds via a coexistent state as a double-peak in $\chi_\perp$ is observed. The fact that the peak in $\chi_=$ at 4.39 ML is coincident with one of the peak positions in $\chi_\perp$ provides additional evidence for the pathway being via a coexistent state. The two peaks in $\chi_\perp$ represent two borders of the coexistent region (points F and G in Fig. 1). The broad peak in $\chi_=$ most likely is a superposition of these peaks. With the boundary conditions described above, we can write down the equations for peaks F and G as:

$$\tilde{K}_1(t_F) + 2K_2(t_F) = 0, \tilde{K}_1(t_G) = 0. \quad (8)$$

For Co/Au(111), 1 ML $\approx$ 0.2 nm.[2] We further take the bulk values for *hcp* Co at room temperature, which are $K_{1b} = 4.1 \times 10^5$ J/m^3, $K_{2b} = 1.5 \times 10^5$ J/m^3, and $M = 1.4 \times 10^6$ A/m.[23] Solving Eq. (8), one obtains $K_{1s} = 7.21 \times 10^{-4}$ J/m^2 and $K_{2s} = -1.43 \times 10^{-4}$ J/m^2 for the Co/Au(111) system. The values agree reasonably well with those estimated by others.[11,23,29]

Furthermore, if the proportion of in-plane/vertical in M components in the coexistent region is available, a quantitative comparison with experimental results can be performed. As an attempt, we first assume that the in-plane M increase linearly with t in the coexistent region. Following the experiments, the *ac* fields $H_=$ and $H_\perp$ are chosen as 0.12 and 0.05 mT, respectively. Figure 4 shows the calculated $\chi(t)$. χ is given in units of ML/mT. To compare with the experimental values, this should be multiplied by the sensitivity according to the technique that used. The calculated χ for $H_\perp$ has peaks at 4.19 and 4.39 ML, while only one broad peak at 4.39 ML is observed for $H_=$. The main features of our calculations

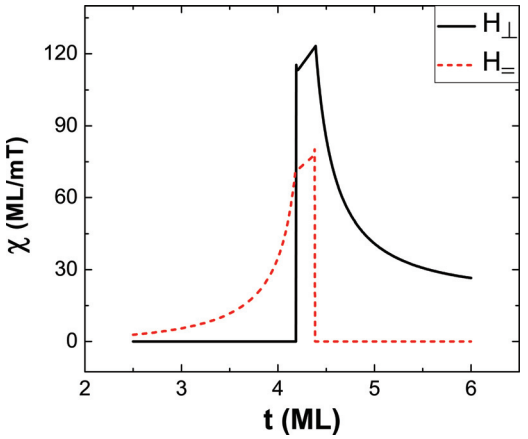

FIG. 4. (Color online) Calculated film thickness dependence of magnetic susceptibilities for Co/Au(111). The *ac* modulation field of 0.12 mT or 0.05 mT is oriented within ($H_=$) or perpendicular to the sample plane ($H_\perp$), respectively.

agree well with experiment. One can also fit the calculated results with the real measurements. This may give information about the occupation of different components of M (perpendicular and in-plane) in the coexistent region.

To further check our model, we consider the influence of external fields on $\chi(t)$ across the SRT. By adding an in-plane *dc* magnetic field, we performed similar calculations as described in the preceding text. In the calculations, the *ac* modulation field (0.16 mT) is applied perpendicular to the sample plane to simulate the experimental configuration. The in-plane magnetization is again assumed to increase linearly with the film thickness. The calculated results are shown in Fig. 5. With increasing the in-plane *dc* bias field, the SRT shifts to lower thickness in comparison with the zero-field configuration. Both susceptibility curves under 50.8 mT/111.3 mT show two peaks with narrower separation. The separation decreases and the peak intensities increase with increasing bias field. The calculated results reproduce the experimental findings, i.e., the SRT shifts to lower thickness and the peak intensity increases with increasing the in-plane bias field. The deviation in peak numbers (two peaks in the calculation and one peak in the

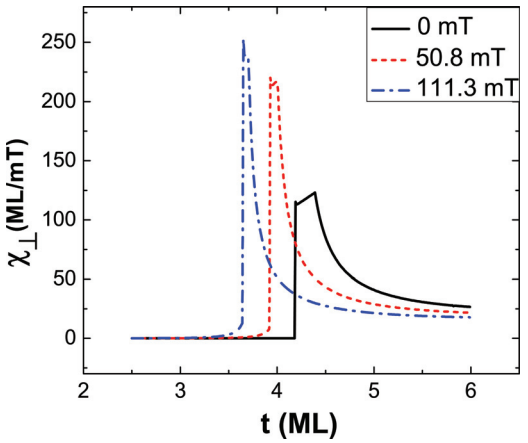

FIG. 5. (Color online) Calculated thickness dependent magnetic susceptibilities for Co/Au(111) in different in-plane *dc* bias fields. The *ac* modulation field of 0.16 mT is applied perpendicular to the sample plane.

TABLE I. Comparison table of several critical thicknesses under different bias fields. t_F and t_G represent the two boundaries of the coexistent region. Calculated values of t_F and t_G are listed for both cases when no in-plane anisotropy and the bulk in-plane anisotropy is included. The last column shows experimental results from Ref. 19.

	Without in-plane anisotropy		With bulk in-plane anisotropy		
Horizontal dc field	t_F (ML)	t_G (ML)	t_F (ML)	t_G (ML)	Exp. (ML)
50.8 mT	3.91	4.01	4.00	4.12	4.11
111.3 mT	3.64	3.71	3.81	3.86	3.90

experiment) may come from the linear assumption we adopted for the magnetization proportionality in the SRT region. The applied *dc* magnetic field can influence the magnetization proportion. When we slightly modified this proportion, the peak at t_F can disappear, while the peak at t_G is less sensitive.

We also list the calculated critical film thicknesses, both t_F and t_G, in different external fields, and the experimental values in Table I. They are in good agreement. The deviation may come from the experimental error margin (0.07 ML)[19] or the assumptions we adopted for the calculation, for instance, neglecting the in-plane anisotropy. When we include the six-fold bulk in-plane anisotropy at room temperature, 6.0×10^3 J/m^3,[30] better agreement is achieved with the experimental values. The peak positions at t_G are shifted to 4.12 ML and 3.86 ML in 50.8 mT and 111.3 mT bias field, respectively (see Table I). The analysis is presented in the following.

Now we discuss the influence of an in-plane anisotropy on SRT. For a hexagonal crystal such as Co(0001), the anisotropy energy can be expressed as:

$$F_A = \tilde{K}_1 \sin^2(\theta) + K_2 \sin^4(\theta) + K_3 \sin^6(\theta)\cos(6\phi), \quad (9)$$

where θ is the angle between the M and the hexagonal axis (for Co/Au(111), it is **n**), and φ is the azimuthal angle of the M.[31] K_3 represents the sixfold in-plane anisotropy constant. When the in-plane anisotropy is included, the equations for the two boundaries of coexistent phase become:

$$\tilde{K}_1(t_F) + 2K_2(t_F) - 3K_3(t_F) = 0, \tilde{K}_1(t_G) = 0. \quad (10)$$

This suggests that the in-plane anisotropy can influence the boundary between the vertical and coexistent state (t_F) but not that between the in-plane and coexistent state (t_G). Therefore the value of $K_{1s} = 7.21 \times 10^{-4}$ J/m^2 remains the same as that obtained without considering the in-plane anisotropy. To obtain the values of K_{2s} and K_3, one more independent equation is needed. The peak position shift caused by the *dc* in-plane bias field can provide such an equation. This is because the in-plane anisotropy can be considered as an effective in-plane field. When both the in-plane *dc* bias field and the in-plane anisotropy are included, it is difficult to obtain analytic solutions. However, numerical calculations can be readily performed. Experimentally, the in-plane field is along the in-plane hard axis.[12,19] We adopt this configuration in the calculations. With a peak position (assumed as t_G) of 4.11 ML for the *dc* bias of 50.8 mT, our calculations show that $K_{2s} = -1.36 \times 10^{-4}$ J/m^2 and $K_3 = 5.6 \times 10^3$ J/m^3. For a peak position (assumed as t_G) of 3.90 ML under 111.3 mT *dc* bias field, we obtain $K_{2s} = -1.32 \times 10^{-4}$ J/m^2 and $K_3 = 8.5 \times 10^3$ J/m^3. The difference of K_3 obtained in distinct bias field may be caused by the linear assumption of the superposition of in-plane and vertical magnetizations, which can influence the peak shift. On the other hand K_3 itself may also depend on t if there is t-dependent strain relief. Nevertheless, these values compare well with the experimental value of 5.5×10^3 J/m^3 for a 6.1±0.3 ML Co film on Au(111)[12] and bulk value 6.0×10^3J/m^3.[30]

IV. SUMMARY

We investigated the susceptibility character of the thickness-driven SRT utilizing the coherent rotation model. We find susceptibilities behave differently for the reorientation transition via a canted state or a coexistent state with increasing film thickness. Also one can extract anisotropy constants from the susceptibility peak positions. When we apply the model to Co/Au(111), we find the thickness-driven SRT in this system proceeds via a state of coexisting phases. The first- and second-order surface/interface anisotropy constants and in-plane anisotropy values obtained are in good agreement with estimates by others.

ACKNOWLEDGMENTS

This work is supported by NSFC (Grants Nos. 10834001, 10874076, 10974087, and 11074112), and the State Key Programme for Basic Research of China (Grants No. 2007CB925104, and 2010CB923401).

[1] H. N. Bertram and M. Williams, IEEE Trans. Magn. **36**, 4 (2000).
[2] L. Cagnon, T. Devolder, R. Cortes, A. Morrone, J. E. Schmidt, C. Chappert, and P. Allongue, Phys. Rev. B **63**, 104419 (2001).
[3] S. Ikeda, K. Miura, H. Yamamoto, K. Mizunuma, H. D. Gan, M. Endo, S. Kanai, J. Hayakawa, F. Matsukura, and H. Ohno, Nat. Mater. **9**, 721 (2010).
[4] C. Liu, E. R. Moog, and S. D. Bader, Phys. Rev. Lett. **60**, 2422 (1988).
[5] N. C. Koon, B. T. Jonker, F. A. Volkening, J. J. Krebs, and G. A. Prinz, Phys. Rev. Lett. **59**, 2463 (1987).
[6] Z. Q. Qiu, J. Pearson, and S. D. Bader, Phys. Rev. Lett. **70**, 1006 (1993).
[7] D. Wilgocka-Ślęzak, K. Freindl, A. Kozioł, K. Matlak, M. Rams, N. Spiridis, M. Ślęzak, T. Ślęzak, M. Zając, and J. Korecki, Phys. Rev. B **81**, 064421 (2010).
[8] R. Allenspach, M. Stampanoni, and A. Bischof, Phys. Rev. Lett. **65**, 3344 (1990).
[9] M. Speckmann, H. P. Oepen, and H. Ibach, Phys. Rev. Lett. **75**, 2035 (1995).
[10] R. Sellmann, H. Fritzsche, H. Maletta, V. Leiner, and R. Siebrecht, Phys. Rev. B **64**, 054418 (2001).
[11] H. P. Oepen, M. Speckmann, Y. Millev, and J. Kirschner, Phys. Rev. B **55**, 2752 (1997).

[12]H. F. Ding, S. Pütter, H. P. Oepen, and J. Kirschner, Phys. Rev. B **63**, 134425 (2001).
[13]B. Schulz and K. Baberschke, Phys. Rev. B **50**, 13467 (1994).
[14]W. L. O'Brien, T. Droubay, and B. P. Tonner, Phys. Rev. B **54**, 9297 (1996).
[15]S. Chikazumi, *Physics of Ferromagnetism* (Oxford University Press, New York, 1997).
[16]A. Berger, S. Knappmann, and H. P. Oepen, J. Appl. Phys. **75**, 5598 (1994).
[17]G. Garreau, E. Beaurepaire, K. Ounadjela, and M. Farle, Phys. Rev. B **53**, 1083 (1996).
[18]C. S. Arnold, D. P. Pappas, and A. P. Popov, Phys. Rev. Lett. **83**, 3305 (1999).
[19]S. Pütter, H. F. Ding, Y. T. Millev, H. P. Oepen, and J. Kirschner, Phys. Rev. B **64**, 092409 (2001).
[20]Y. Millev and J. Kirschner, Phys. Rev. B **54**, 4137 (1996).
[21]Y. T. Millev, H. P. Oepen, and J. Kirschner, Phys. Rev. B **57**, 5837 (1998).
[22]U. Gradmann and J. Müller, Phys. Stat. Sol. **27**, 313 (1968).
[23]*Ultrathin Magnetic Structures*, edited by J. A. C. Bland and B. Heinrich (Springer, Berlin, 1994), Vol. I.
[24]A. P. Popov, N. V. Skorodumova, and O. Eriksson, Phys. Rev. B **77**, 014415 (2008).
[25]Z. Q. Qiu, J. Pearson, and S. D. Bader, Phys. Rev. B **46**, 8195 (1992).
[26]Y. Z. Wu, C. Won, A. Scholl, A. Doran, H. W. Zhao, X. F. Jin, and Z. Q. Qiu, Phys. Rev. Lett. **93**, 117205 (2004).
[27]H. P. Oepen, Y. T. Millev, H. F. Ding, S. Pütter, and J. Kirschner, Phys. Rev. B **61**, 9506 (2000).
[28]H. F. Ding, S. Pütter, H. P. Oepen, and J. Kirschner, J. Magn. Magn. Mater. **212**, L5 (2000).
[29]H. Fritzsche, J. Kohlhepp, and U. Gradmann, J. Magn. Magn. Mater. **148**, 154 (1995).
[30]M. B. Stearns, *Magnetic Properties of Metals*, edited by H. P. J. Wijn, Landolt-Börnstein (Springer-Verlag, New York, 1986), New Series, Group III, Vol. 19a, Pt. 1.1.2.
[31]*Ultrathin Metal Films*, edited by M. Wuttig and X. D. Liu (Springer, Berlin, 2004).